European Journal of Cancer 132 (2020) 24–34

Available online at www.sciencedirect.com

ScienceDirect

journal homepage: www.ejcancer.com

Original Research

An immune gene expression signature distinguishes central nervous system metastases from primary tumours in non–small-cell lung cancer

Georgios Tsakonas [a,b], Rolf Lewensohn [a,b], Johan Botling [c], Cristian Ortiz-Villalon [b], Patrick Micke [c], Signe Friesland [a,b], Helena Nord [d], Magnus Lindskog [e], Martin Sandelin [f], Per Hydbring [b,1], Simon Ekman [a,b,*,1]

[a] *Thoracic Oncology Center, Karolinska University Hospital, Stockholm, Sweden*
[b] *Department of Oncology and Pathology, Karolinska Institutet, Visionsgatan 4, 17164 Stockholm, Sweden*
[c] *Department of Immunology, Genetics and Pathology, Uppsala University, Uppsala Sweden*
[d] *Department of Immunology, Genetics and Pathology and Science for Life Laboratory, Uppsala University, Uppsala, Sweden*
[e] *Department of Immunology, Genetics and Pathology, Uppsala University/Department of Oncology, Uppsala University Hospital, Sweden*
[f] *Department of Medical Sciences, Uppsala University/ Department of Oncology, Uppsala University Hospital, Sweden*

Received 19 January 2020; received in revised form 8 March 2020; accepted 18 March 2020
Available online 20 April 2020

KEYWORDS
Immune signature;
Gene expression;
Brain metastases;
Non–small-cell lung cancer;
Matched analyses

Abstract ***Background:*** Dissemination of non–small-cell lung cancer (NSCLC) in the central nervous system is a frequent and challenging clinical problem. Systemic or local therapies rarely prolong survival and have modest activity regarding local control. Alterations in gene expression in brain metastasis versus primary tumour may increase aggressiveness and impair therapeutic efforts.

Methods: We identified 25 patients with surgically removed NSCLC brain metastases in two different patient cohorts. For 13 of these patients, primary tumour samples were available. Gene expression analysis using the nCounter® PanCancer Immune Profiling gene expression panel (nanoString technologies Inc.) was performed in brain metastases and primary tumour samples. Identification of differentially expressed genes was conducted on normalized data using the nSolver analysis software.

Results: We compared gene expression patterns in brain metastases with primary tumours. Brain metastasis samples displayed a distinct clustering pattern compared to primary tumour

* *Corresponding author*: Thoracic Oncology Center, Karolinska University Hospital/Department of Oncology-Pathology, Karolinska Institutet, 17176, Stockholm, Sweden.
E-mail address: simon.ekman@ki.se (S. Ekman).
[1] Shared last authors.

https://doi.org/10.1016/j.ejca.2020.03.014

samples with a statistically significant downregulation of genes related to immune response and immune cell activation. Results from KEGG term analysis on differentially expressed genes revealed a concomitant enrichment of multiple KEGG terms associated with the immune system. We identified a 12-gene immune signature that clearly separated brain metastases from primary tumours.

Conclusions: We identified a unique gene downregulation pattern in brain metastases compared with primary tumours. This finding may explain the lower intracranial efficacy of systemic therapy, especially immunotherapy, in brain metastasis of patients with NSCLC.

1. Introduction

Brain metastases (BMs) are common in advanced non–small-–cell lung cancer (NSCLC) [1]. Brain dissemination occurs more frequently in patients with adenocarcinoma and especially in patients with oncogenic-driven tumours. The incidence of BM appears to be increasing mostly owing to improvements in diagnostic imaging and in survival associated with more effective systemic therapies. Approximately 45% of patients with advanced NSCLC and up to 70% of patients with *EML4-ALK* rearrangements or *EGFR* mutations, will be diagnosed with BM during the course of the disease [1–3]. Patients with NSCLC with BM have a poor prognosis with 4–11 weeks median overall survival in untreated patients and 4–15 months in patients who receive treatment [4].

Prognosis is significantly better in patients with oncogenic-driven tumours and BM, where high response rates and prolonged survival can be achieved with the use of targeted therapies, including against EGFR and ALK [5,6]. However, targeted therapies only apply to a smaller proportion of patients with lung cancer. Treatment of BM in non-oncogenic–driven NSCLC is a challenging clinical issue because there are limited treatment options that can prolong survival, and the toxicity related to these treatments is often considerable. Chemotherapy can achieve intracranial response rates of 20–45%, albeit only in selected patients who can receive platinum-doublet regimens upfront [7,8]. Besides surgery for single BM in patients without evidence of extracranial tumour activity, there are no other local central nervous system (CNS) therapies that have shown a clear survival benefit [9]. Salvage chemotherapy after local CNS treatment provides a modest clinical benefit [10]. Immunotherapy using immune checkpoint inhibitors (ICIs) has started a new era of treatment for lung cancer. Numerous studies in both second and first line have demonstrated improved survival of patients with NSCLC receiving PD-1/PD-L1 inhibitors versus chemotherapy [11–13] or in combination with chemotherapy versus chemotherapy in first-line [14,15]. However, for the subgroup of patients with brain metastasis evidence is scarcer regarding the efficacy of ICIs and the use of ICIs in these patients still remains a matter of debate.

In our study, gene expression analysis was carried out from formalin-fixed, paraffin-embedded (FFPE) tissue sections of primary lung tumours and matched brain metastases. The aim was to identify potential patterns of gene downregulation or upregulation in the BM setting that could potentially explain the dismal prognosis of these patients, function as a diagnostic tool and constitute new treatment strategies.

2. Material and methods

2.1. Patient cohort

We identified patients with lung cancer with surgically removed BM from two cohorts.

The first cohort consisted of 725 patients with surgically removed NSCLC and the second of 280 patients who had received whole brain radiotherapy during the course of their disease. Both cohorts are described in previous publications [16,17]. We analysed a total of 43 tissue samples for systematic mRNA expression; 13 primary tumours and 30 brain metastases. The material was obtained from 25 patients, of which 13 underwent surgery of the primary tumour. The paired samples were 26 (13 patients with both available lung and brain tissue samples).

2.2. Sample preparation

Total RNA was isolated from FFPE tissue sections of primary tumours and matched brain metastases using RNeasy FFPE kit (Qiagen, Hilden, Germany) in accordance with manufacturers' instructions. Tissue sections of 4 × 4 μm were used. RNA quantity and quality were assessed using RNA Screen Tapes on a 2200 TapeStation system (Agilent, Santa Clara, CA, USA) through the documentation of RNA integrity number curves. All tissue samples selected for preparation displayed similar RNA integrity number curves.

2.3. mRNA expression analysis

Systematic mRNA expression was measured on an nCounter FLEX™ Analysis System (nanoString, Seattle, WA, USA) using the nCounter® PanCancer Immune Profiling gene expression panel (nanoString technologies Inc.), covering 770 human mRNAs associated to tumour and immunity-related pathways. A minimum input of 150 ng of total RNA was used for each sample. Fluorescently colour-coded reporter probes and biotin-labelled capture probes were hybridized to the mRNA on a thermal cycler overnight and automatically processed and loaded to the nanoString provided sample cartridge in the nCounter Prep Station in accordance with the manufacturer's protocol.

2.4. Statistical analysis

mRNA expression normalization, hierarchical clustering, scatter plots, fold-changes and statistical ranking of differentially expressed genes, along with FDR corrected p-values, were performed using the nanoString nSolver analysis software (nanoString technologies Inc.). mRNA raw expression counts were normalized to the top 100 genes. Hierarchical clustering was performed using Euclidean distance with average linkage. Normalized expression values of the top twelve differentially expressed mRNAs were extracted from all samples. Scatter plots and curves displaying receiver operating characteristics (ROCs) along with values for area under curve (AUC) were acquired using Graphpad Prism 8. All differentially expressed genes were subjected to KEGG term analysis, including calculation of Benjamini-Hochberg corrected p-values, through the miRWalk 3.0 software. Visualization of KEGG gene interaction networks was performed through the NetworkAnalyst 3.0 software. Specifically, the node network was visualized through the layout settings 'Force Atlas' and 'Reduce Overlap'.

Descriptive statistic was used for the demographic and clinical characterization of the cohort. Univariate Cox regression analyses were undertaken with performance status (PS), age at diagnosis, histology, received oncologic treatment, stage of disease at lung cancer diagnosis, CNS metastasis at diagnosis, gender, number of CNS metastases, recursive partitioning analysis (RPA) class and graded prognostic assessment (GPA) score as independent variables. All these statistical analyses were carried out with SPSS version 23.

2.5. Ethics statement

The study has received ethical approval by the institutional review board at Karolinska University Hospital (Registration number: 2016/944-31/1). An additional approval by Stockholms Biobank was received (Bbk-01605). At the time of data analysis and sample collection, all patients were deceased; therefore no patient informed consent deemed necessary from the previously mentioned authorities.

3. Results

3.1. Patient characteristics

The demographics and disease characteristics of the whole cohort are presented in Table 1. The most common sex was male (64%) and histology adenocarcinoma (68%). None of the patients received whole brain radiotherapy (WBRT) or stereotactic radiosurgery (SRS) before surgery in the CNS. None of the patients received systemic therapy between the diagnosis of brain metastasis and surgery in the CNS. The most common RPA and GPA groups were 2 for both, 56% and 64%, respectively (RPA class and GPA score are explained in Supplementary Table 1). The univariate Cox regression analysis for clinical and demographic variables showed that sex, brain metastasis at diagnosis, RPA class, PS

Table 1
Baseline demographics and disease characteristics.

Variable	n (%)
Gender (male)	16 (64)
Age (mean ± SD)	62 ± 7.8
Histology (%)	
- Adenocarcinoma	17 (68)
- Squamous cell	4 (16)
- SCLC	1 (4)
- Large cell	3 (12)
WHO performance status	
0–1	20 (80)
2	4 (16)
3	1 (4)
CNS metastasis at diagnosis	6 (24)
Oncologic therapy	
Surgery primary tumour	13 (52)
Systemic therapy	20 (80)
CNS radiotherapy	23 (92)
GPA class group (%)	
1 (0–1)	7 (28)
2 (1.5–2.5)	14 (56)
3 (3,4)	4 (16)
RPA class (%)	
1	5 (20)
2	16 (64)
3	4 (16)
Number of CNS metastases (%)	
1	10 (40)
2–3	7 (28)
>3	8 (32)
Stage at diagnosis	
I	5 (20)
II	2 (8)
III	10 (40)
IV	8 (32)

RPA, recursive partitioning analysis; GPA, graded prognostic assessment; CNS, central nervous system; SCLC, small-cell lung cancer; SD, standard deviation.

and number of brain metastasis had prognostic value (Supplementary Table 2).

3.2. Gene expression analysis

The fraction of tumour cells was generally slightly higher in the brain metastases samples than the primary tumours with a range of 30–50% tumour cells in brain metastases (mean: 43%) and 20–50% in primary tumours (mean: 31%) (data not shown). Samples were divided into two groups, primary and CNS metastasis, and subjected to mRNA array analysis using the nanoString Pan-Cancer Immune Oncology panel followed by ranking of transcripts with differential expression between the groups. The expression of 208 mRNAs (of 770) was statistically significantly altered (FDR corrected p-value <0.05) when comparing primary tumours with brain metastatic lesions. Intriguingly, all differentially expressed transcripts displayed decreased expression in brain metastases, but with a large variation in relative fold-changes (1.43–96.70 fold expression in primary tumour compared with brain metastases) (Supplementary Table 3). In concordance with the fraction of differentially expressed genes, brain metastases samples largely clustered in a distinct manner compared to samples from primary tumours (Fig. 1A). This pattern was substantiated when only including genes with a corrected p-value of <0.01 (Fig. 1B), or when specifically selecting the top twelve most differentially expressed genes (Fig. 1C). Selecting the top twelve most differentially expressed genes for hierarchical clustering resulted in two main clustering arms, covering 17 and 26 samples, respectively. All 13 primary samples were located in the first clustering arm, whereas 26 of 30 brain metastases samples were located in the second clustering arm (Fig. 1C). As seen from the analysis of differentially expressed genes, brain metastases samples exhibited an overall decreased cancer mRNA expression compared to primary samples (Fig. 1A–C). Owing to the non-balanced number of primary tumour samples versus brain metastases samples, we analysed the mRNA expression of all genes from patients which had available both a primary tumour and a brain metastasis sample. As reflected in Fig. 2, mRNA expression was largely decreased in the brain metastatic lesion, compared with the primary tumour, irrespective of investigated patient. Moreover, top differentially expressed genes, CCL19 and CCL21, were substantially dampened in the brain metastatic lesion (Fig. 2A–H). Of the top twelve most differentially expressed mRNAs, seven belonged to the chemokine (CCL19, CCL21, CXCL9, CCL14, CCL18) or cytokine-receptor families (IL2RB, IL21R). The additional five most differentially expressed transcripts were CD48, GZMA, ITGA4, RUNX3 and TPSAB1. All transcripts displayed some variety in normalized expression within the analysed groups (Fig. 3A-L). By analysing mean transcript expression, primary tumours were distinguished from brain metastatic lesions most clearly by CCL19 and CCL21 (Fig. 3A and B). To evaluate whether differential expression translated into diagnostic power, we investigated the diagnostic performance of our top differentially expressed mRNAs, by computing their ROC scores, where an AUC value higher than 0.95 represents an excellent diagnostic performance (Fig. 4A-L). The best performing individual transcript was CCL19 with an AUC score of 0.9795 (Fig. 4A), followed by CCL21 with an AUC score of 0.9667 (Fig. 4B). In total, four transcripts scored an AUC >0.95 (CCL19, CCL21, IL2RB and TPSAB1). All top twelve differentially expressed transcripts scored an AUC >0.90 (Fig. 4A-L).

3.3. Pathway analysis

Finally, we performed an *in silico* pathway association of all transcripts being differentially expressed in brain metastatic lesions, by computing their KEGG term associations. Our analysis generated a total of 35 KEGG terms with a highly significant p-value ($p < 0.0001$, Benjamini-Hochberg corrected). Of these KEGG terms, 'Cytokine-cytokine receptor interaction' attracted the highest number of differentially expressed transcripts, 56, of which seven were found among the top twelve differentially expressed transcripts (Supplemental Table 4). By subjecting our statistically differentially expressed mRNA transcripts to KEGG term node-network visualization, we unveiled two major KEGG-networks (Fig. 5), harbouring 31 and 24 statistically significant KEGG terms, respectively.

4. Discussion

A unique gene downregulation pattern in the brain metastatic setting was identified in this cohort of patients with matched gene expression analyses from primary lung cancer and brain metastasis. These genes either belong to the cytokine and chemokine receptor families or are otherwise involved in immune response and immune cell activation. For example, we observed statistically significant downregulation of several genes encoding for checkpoint proteins, including PDCD1 (encoding the PD-1 protein), CTLA4, LAG3 and ICOS [18], all with >3 fold-expression in primary tumour compared to BM (Supplemental Table 3).

Chemokines are secreted proteins that recruit and are essential for the function of immune cells. In this way, chemokines can contribute to an 'inflamed' tumour microenvironment permissive of a response to ICIs. The most differentially expressed genes in our study, CCL19 and CCL21, recruit Tregs, CD4 T-helper and activated T-cells, monocyte-derived dendritic cells and B-cells to

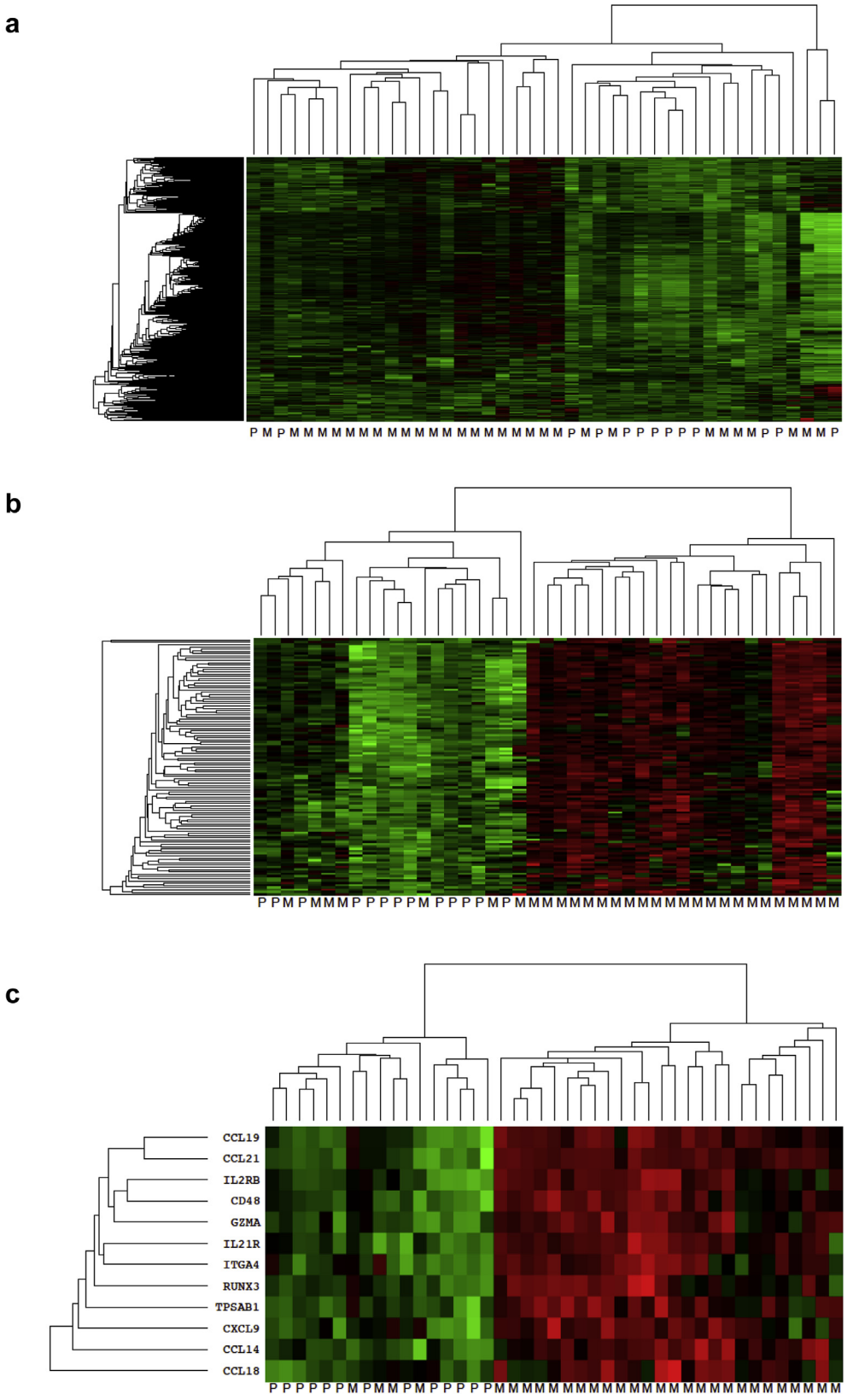

Fig. 1. Expression of immune oncology mRNA transcripts is substantially altered in metastatic lesions versus lung primary tumours. (a) Unsupervised hierarchical clustering of 770 mRNAs from 13 lung primary tumours and 30 metastatic lesions. (b) Hierarchical clustering of differentially expressed mRNA transcripts (FDR <0.01) between 13 lung primary tumours and 30 metastatic lesions. (c) Hierarchical clustering of the top twelve most differentially expressed transcripts between 13 lung primary tumours and 30 metastatic lesions. Columns represent individual biological samples. Rows represent individual mRNA transcripts. Expression is displayed on a log 10-scale from red (low expression) to green (high expression). P = primary tumour. M = metastatic lesion.

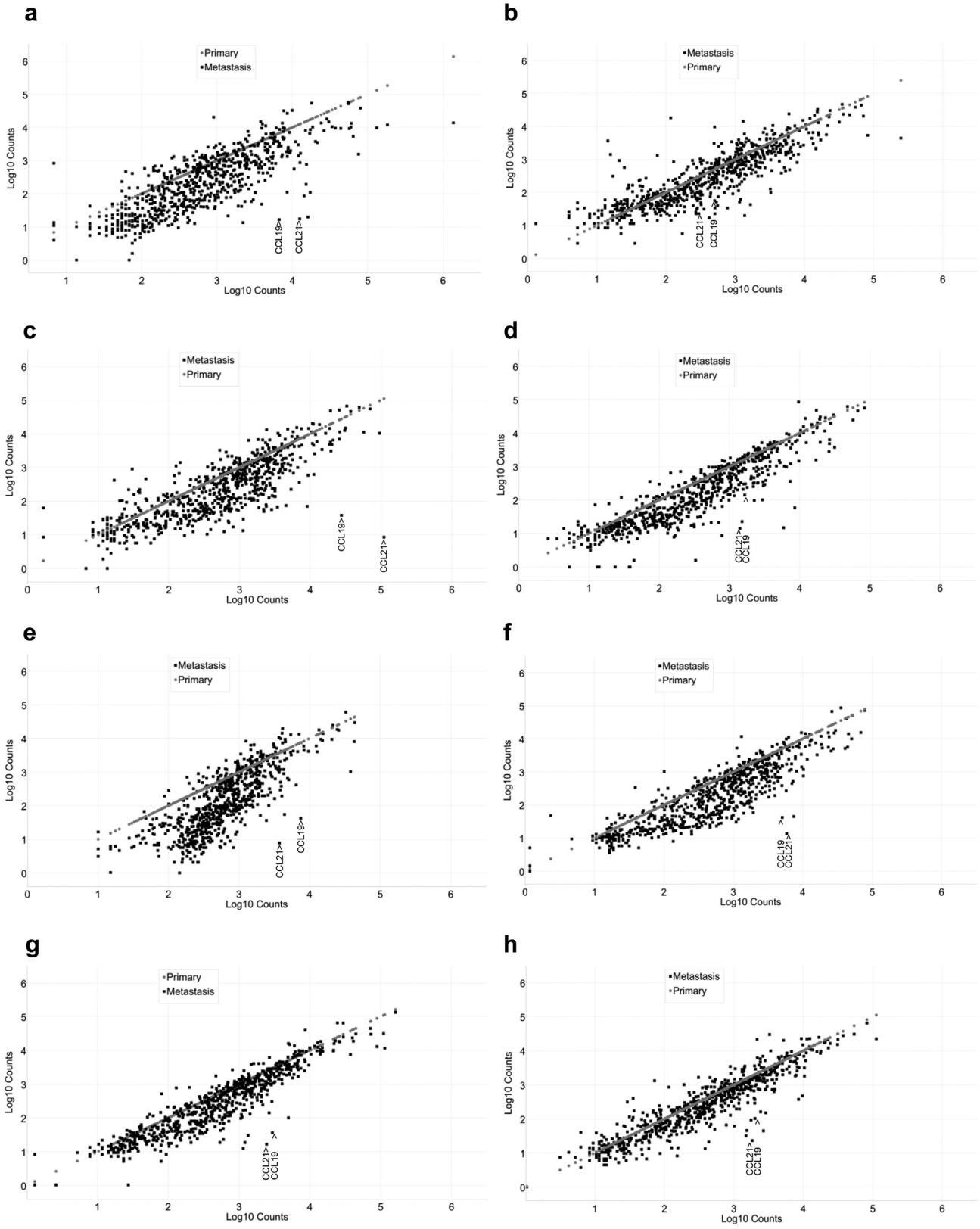

Fig. 2. Profiling of immune oncology mRNA transcripts in individual patients with metastatic disease. (a–h) Normalized mRNA expression is displayed for 770 mRNA transcripts in eight patients with primary lung tumours (linear grey dotted line) and metastatic lesions (black squares). Each data point represents one mRNA transcript. Expression is displayed on a log 10-scale. Expression of CCL19 and CCL21 in the metastatic lesion is indicated. Y-axis: Expression of transcripts from metastatic lesions. X-axis: Expression of transcripts from primary lung tumours.

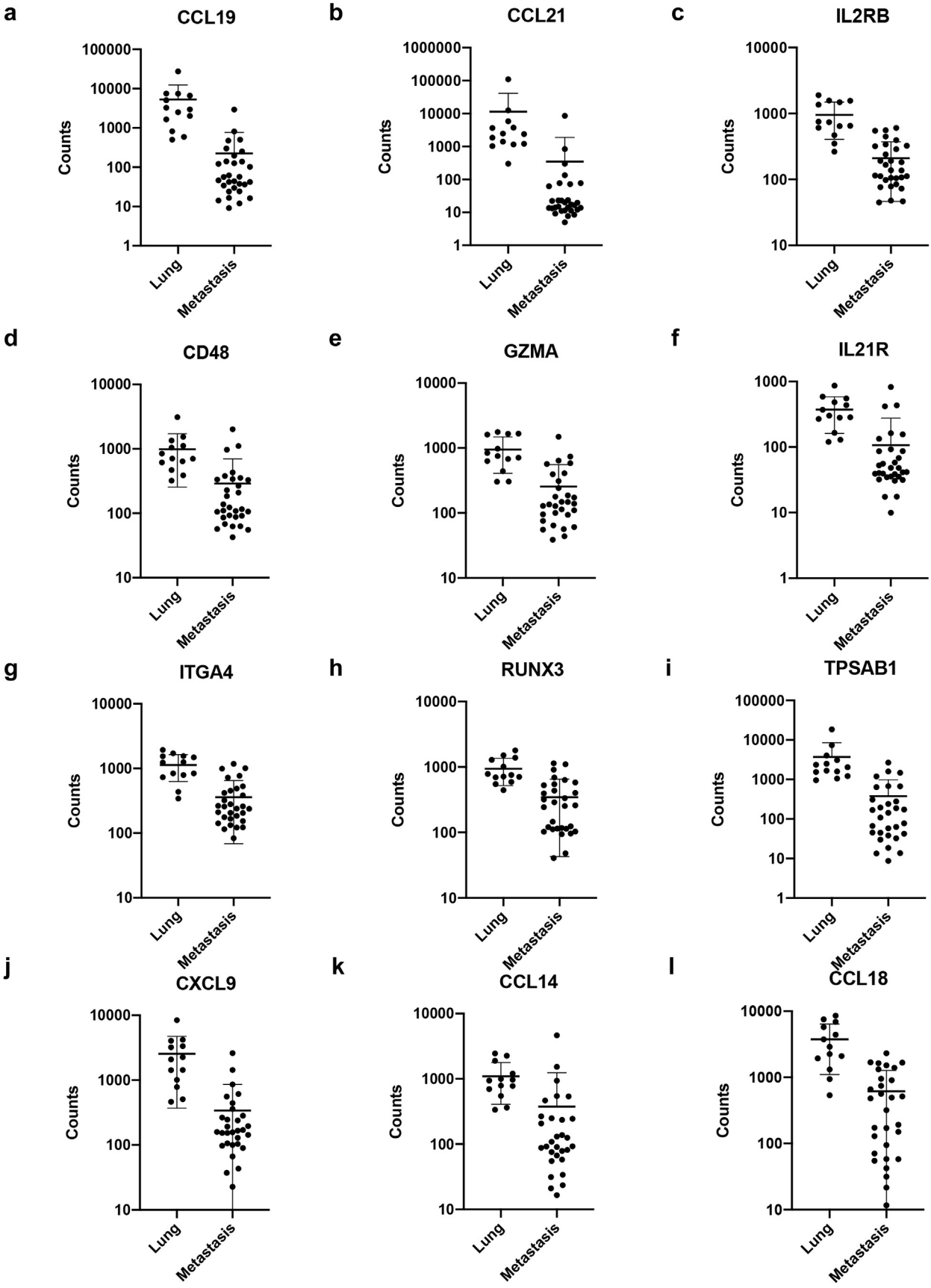
a
CCL19
b
CCL21
c
IL2RB
d
CD48
e
GZMA
f
IL21R
g
ITGA4
h
RUNX3
i
TPSAB1
j
CXCL9
k
CCL14
l
CCL18
Counts
Lung
Metastasis

the tumour microenvironment through interaction with the chemokine receptor CCR7, another differentially expressed gene in our cohort of primary lung cancer and BM (Supplemental Table 3) [19]. The deregulation of these immune checkpoints used as targets for therapy further confirms our findings of a general immune suppressed profile of brain metastases. This may open up for new treatment strategies of brain metastases in NSCLC where modulation of chemokine and cytokine signalling can be used to create an 'immune-rich' tumour microenvironment optimized for a response to ICIs.

This differential gene expression was evaluated with ROC scores, where an excellent diagnostic performance was observed for 12 genes. This 12-gene signature clearly separated brain metastases from primary tumours and may be used in the diagnosis of NSCLC BM in the clinical setting where several applications are possible. The diagnosis of BM may sometimes be challenging with several possible differential diagnoses, including infections, and the signature may be an aid in the diagnostic work. However, the diagnosis is often hindered by the difficulty in obtaining diagnostic material from the brain metastasis, and it remains to be seen if the 12-gene signature identified in our study (Figs. 1C, Figs. 3–4) is reflected in the cerebrospinal fluid compartment, or even in blood, from patients with NSCLC with BM. Another diagnostic application of the signature may be to monitor patients during treatment to assess treatment response, including to immunotherapy.

The hypothesis that brain metastases differ molecularly from primary tumours has been suggested by other studies. In one of the largest trials, which addressed this issue, whole-exome sequencing was performed in 86 patients with paired brain metastasis, primary tumour and normal tissue. In 53% of cases, potentially clinically informative alterations in the brain metastasis not detected in the matched primary tumour sample were found. In contrast, separated brain metastatic sites from individual cases were genetically homogenous [20]. A similar study using next generation sequencing in paired samples from 79 patients with squamous cell lung cancer also showed genetic heterogeneity between brain metastasis and primary tumour [21]. There is scarce data regarding gene expression analysis in paired brain metastasis and primary tumour samples from patients with lung cancer. A recently published trial by Kudo *et al.* [22] included paired gene expression analyses in patients with brain metastasis and primary tumour samples and showed an immunosuppression of the tumour microenvironment in brain metastasis compared with the primary tumour.

One limitation of our study is that we did not perform sequencing to identify relevant mutations and correlate mutations with gene expression. Another limitation is that no specific analyses were performed of the tumour microenvironment, but rather in the whole tumour making it difficult to distinguish the contribution of tumour cells vs. surrounding stromal cells to the gene expression profiles. In the study by Kudo *et al.* [22] mentioned previously, it was shown that the immune microenvironment of brain metastasis is overall immunosuppressed. The results of our study validate this finding beacuse the specific gene downregulation observed is reflective of an immunosuppressive environment in the brain metastatic setting.

The fraction of tumour cells was generally slightly higher in the brain metastases samples compared to the primary tumours with a range of 30–50% tumour cells in brain metastases (mean: 43%) and 20–50% in primary tumours (mean: 31%). This finding is expected because metastases often contain a purer fraction of tumour cells compared with primary lung tumours which often are heterogeneous containing a substantial fraction of tumour stroma. The fraction of immune cells was not evaluated in this study. The finding of downregulated genes in brain metastases should then not be explained by a lower fraction of tumour cells in the metastases.

The results from our study may explain the low intracranial response rates and the limited efficacy of ICIs for patients with brain metastatic NSCLC. Interestingly, multiple genes encoding for immune checkpoint proteins displayed substantially dampened expression in the brain metastases samples compared to primary tumour (Supplemental Table 3). The deregulation of immune checkpoint proteins used as targets for therapy further confirm our findings of a general immune suppressed profile of brain metastases. This may open up for new treatment strategies of brain metastases in NSCLC where modulation of chemokine and cytokine signalling can be used to create an 'immune-rich' tumour microenvironment optimized for a response to ICIs. The registration trials evaluating single ICI for advanced NSCLC have included small numbers of asymptomatic brain metastatic patients and data from such subgroup analyses, as well as from retrospective series have shown limited activity of ICI in brain metastatic NSCLC [23–27]. To achieve higher response rates in the CNS, new treatment strategies are needed. Combination treatments with two different ICIs, or ICI

Fig. 3. Reduced abundance of multiple chemokines and cytokine-receptors classify brain metastases. (a–l) Normalized expression counts for CCL19 (a), CCL21 (b), IL2RB (c), CD48 (d), GZMA (e), IL21R (f), ITGA4 (g), RUNX3 (h), TPSAB1 (i), CXCL9 (j), CCL14 (k) and CCL18 (l) are displayed for primary lung tumours (Lung) versus brain metastatic lesions (Metastasis). Expression is displayed on a logarithmic scale. Each data point represents one biological sample.

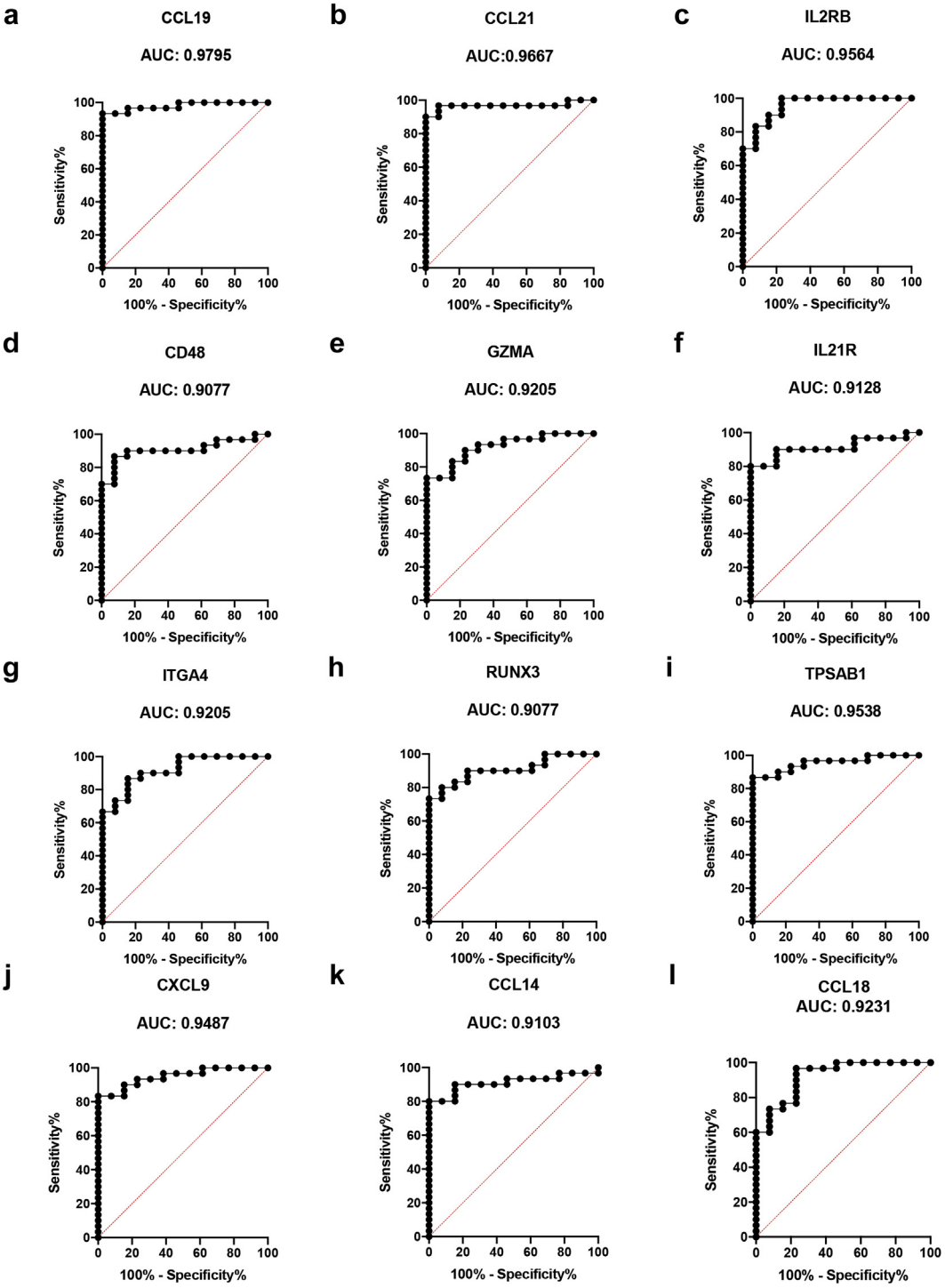

Fig. 4. Diagnostic performance of top differentially expressed mRNAs. (a–l) ROC-curves and AUC-scores for mRNAs CCL19 (a), CCL21 (b), IL2RB (c), CD48 (d), GZMA (e), IL21R (f), ITGA4 (g), RUNX3 (h), TPSAB1 (i), CXCL9 (j), CCL14 (k) and CCL18 (l) based on normalized expression counts. Each dot is derived from the signal of a sample probe. ROC, receiver operating characteristic; AUC, area under curve.

and other drugs influencing the immune microenvironment/immune cells in the CNS, seem to be a reasonable approach [28,29].

In conclusion, we identified a unique gene down-regulation pattern in brain metastatic NSCLC samples compared with primary tumours, especially regarding genes related to immune response and immune cell activation. This finding may explain the lower clinical efficacy of systemic therapy, especially immunotherapy, in brain metastasis of patients with NSCLC and opens

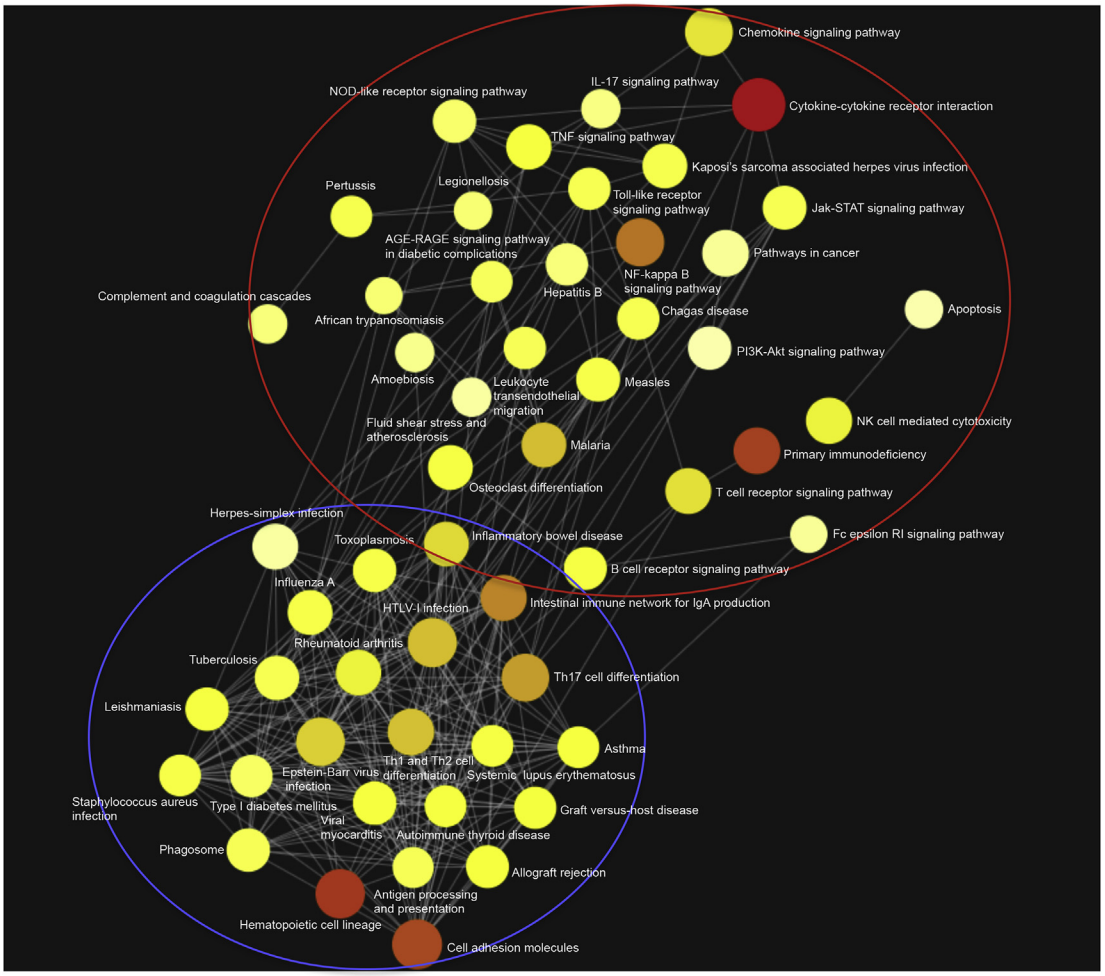

Fig. 5. Differentially expressed mRNA transcripts associates to immunity-related pathways. Each circle represents one KEGG-term. All circles are connected through nodes to their closest associated neighbour. Circle size represents the number of differentially expressed mRNA transcripts. Statistical significance (Benjamini-Hochberg corrected) of each KEGG-term is displayed on a colour scale from white (lower significance) to red (higher significance).

up for new treatment strategies. Furthermore, a 12-gene signature with excellent diagnostic performance for brain metastatic NSCLC was identified and will be subject for further validation studies in other patient cohorts.

Funding

This work was supported by Stockholm Cancer Society, Sweden, grant number 174093, and the Lion Cancer Fund in Uppsala, Sweden.

Conflict of interest statement

Nothing declared.

Acknowledgements

This work was supported by Stockholm Cancer Society (grant number 174093) and the Lion Cancer Fund in Uppsala. Role of the funding sources: provided unrestricted funding for this academic research project.

Appendix A. Supplementary data

Supplementary data to this article can be found online at https://doi.org/10.1016/j.ejca.2020.03.014.

References

[1] Doebele RC, Lu X, Sumey C, Maxson DA, Weickhardt AJ, Oton AB, et al. Oncogene status predicts patterns of metastatic spread in treatment-naive nonsmall cell lung cancer. Cancer 2012; 118(18):4502–11.
[2] Ge M, Zhuang Y, Zhou X, Huang R, Liang X, Zhan Q. High probability and frequency of EGFR mutations in non-small cell lung cancer with brain metastases. J Neuro Oncol 2017;135(2):413–8.
[3] Shin DY, Na II, Kim CH, Park S, Baek H, Yang SH. EGFR mutation and brain metastasis in pulmonary adenocarcinomas. J Thorac Oncol : offl Publ Int Assoc Study Lung Cancer 2014;9(2): 195–9.

[4] Besse B, Le Moulec S, Mazieres J, Senellart H, Barlesi F, Chouaid C, et al. Bevacizumab in patients with nonsquamous non-small cell lung cancer and asymptomatic, untreated brain metastases (brain): a nonrandomized, phase II study. Clin Canc Res : Offl J Am Assoc Cancer Res 2015;21(8):1896–903.
[5] Gadgeel SM, Shaw AT, Govindan R, Gandhi L, Socinski MA, Camidge DR, et al. Pooled analysis of CNS response to alectinib in two studies of pretreated patients with ALK-positive non–small-cell lung cancer. J Clin Oncol 2016 Dec;34(34):4079–85.
[6] Soria JC, Ohe Y, Vansteenkiste J, Reungwetwattana T, Chewaskulyong B, Lee KH, et al. Osimertinib in untreated EGFR-mutated advanced non-small-cell lung cancer. N Engl J Med 2018;378(2):113–25.
[7] Bernardo G, Cuzzoni Q, Strada MR, Bernardo A, Brunetti G, Jedrychowska I, et al. First-line chemotherapy with vinorelbine, gemcitabine, and carboplatin in the treatment of brain metastases from non-small-cell lung cancer: a phase II study. Canc Invest 2002;20(3):293–302.
[8] Cortes J, Rodriguez J, Aramendia JM, Salgado E, Gurpide A, Garcia-Foncillas J, et al. Front-line paclitaxel/cisplatin-based chemotherapy in brain metastases from non-small-cell lung cancer. Oncology 2003;64(1):28–35.
[9] Kalkanis SN, Kondziolka D, Gaspar LE, Burri SH, Asher AL, Cobbs CS, et al. The role of surgical resection in the management of newly diagnosed brain metastases: a systematic review and evidence-based clinical practice guideline. J Neuro Oncol 2010; 96(1):33–43.
[10] Kelly K, Bunn Jr PA. Is it time to reevaluate our approach to the treatment of brain metastases in patients with non-small cell lung cancer? Lung cancer 1998;20(2):85–91.
[11] Borghaei H, Paz-Ares L, Horn L, Spigel DR, Steins M, Ready NE, et al. Nivolumab versus docetaxel in advanced non-squamous non-small-cell lung cancer. N Engl J Med 2015;373(17): 1627–39.
[12] Brahmer J, Reckamp KL, Baas P, Crino L, Eberhardt WE, Poddubskaya E, et al. Nivolumab versus docetaxel in advanced squamous-cell non-small-cell lung cancer. N Engl J Med 2015; 373(2):123–35.
[13] Reck M, Rodriguez-Abreu D, Robinson AG, Hui R, Csoszi T, Fulop A, et al. Pembrolizumab versus chemotherapy for PD-L1-positive non-small-cell lung cancer. N Engl J Med 2016;375(19): 1823–33.
[14] Paz-Ares L, Luft A, Vicente D, Tafreshi A, Gümüş M, Mazières J, et al. Pembrolizumab plus chemotherapy for squamous non-small-cell lung cancer. N Engl J Med 2018;379(21): 2040–51.
[15] Gandhi L, Rodríguez-Abreu D, Gadgeel S, Esteban E, Felip E, De Angelis F, et al. Pembrolizumab plus chemotherapy in metastatic non-small-cell lung cancer. N Engl J Med 2018;378(22): 2078–92.
[16] Tsakonas G, Botling J, Micke P, Rivard C, LaFleur L, Mattsson J, et al. c-MET as a biomarker in patients with surgically resected non-small cell lung cancer. Lung cancer 2019; 133:69–74.
[17] Tsakonas G, De Petris L, Ekman S. Management of brain metastasized non-small cell lung cancer (NSCLC) - from local treatment to new systemic therapies. Canc Treat Rev 2017;54: 122–31.
[18] Pardoll DM. The blockade of immune checkpoints in cancer immunotherapy. Nat Rev Canc 2012;12(4):252–64.
[19] Vilgelm AE, Richmond A. Chemokines modulate immune surveillance in tumorigenesis, metastasis, and response to immunotherapy. Front Immunol 2019;10:333.
[20] Brastianos PK, Carter SL, Santagata S, Cahill DP, Taylor-Weiner A, Jones RT, et al. Genomic characterization of brain metastases reveals branched evolution and potential therapeutic targets. Canc Discov 2015;5(11):1164–77.
[21] Paik PK, Shen R, Won H, Rekhtman N, Wang L, Sima CS, et al. Next-generation sequencing of stage IV squamous cell lung cancers reveals an association of PI3K aberrations and evidence of clonal heterogeneity in patients with brain metastases. Canc Discov 2015;5(6):610–21.
[22] Kudo Y, Haymaker C, Zhang J, Reuben A, Duose DY, Fujimoto J, et al. Suppressed immune microenvironment and repertoire in brain metastases from patients with resected non-small-cell lung cancer. Ann Oncol : Offl J European Soc Med Oncology/ESMO 2019;30(9):1521–30.
[23] Dudnik E, Yust-Katz S, Nechushtan H, Goldstein DA, Zer A, Flex D, et al. Intracranial response to nivolumab in NSCLC patients with untreated or progressing CNS metastases. Lung cancer 2016;98:114–7.
[24] Goldberg SB, Gettinger SN, Mahajan A, Chiang AC, Herbst RS, Sznol M, et al. Pembrolizumab for patients with melanoma or non-small-cell lung cancer and untreated brain metastases: early analysis of a non-randomised, open-label, phase 2 trial. Lancet Oncol 2016;17(7):976–83.
[25] Crinò L, Bidoli P, Ulivi P, Minenza E, Cortesi E, Garassino M, et al. P1.01-053 Italian nivolumab expanded access programme (EAP): data from patients with advanced non-squamous NSCLC and brain metastases. J Thorac Oncol 2017;12(11):S1915.
[26] Geier M, Descourt R, Corre R, Léveiller G, Lamy R, Goarant E, et al. MA08.10 real-life intracerebral efficacy of nivolumab in non-small cell lung cancer patients with brain metastases. J Thorac Oncol 2018;13(10):S384–5.
[27] Gauvain C, Vauleon E, Chouaid C, Le Rhun E, Jabot L, Scherpereel A, et al. Intracerebral efficacy and tolerance of nivolumab in non-small-cell lung cancer patients with brain metastases. Lung cancer 2018;116:62–6.
[28] Long GV, Atkinson V, Lo S, Sandhu S, Guminski AD, Brown MP, et al. Combination nivolumab and ipilimumab or nivolumab alone in melanoma brain metastases: a multicentre randomised phase 2 study. Lancet Oncol 2018;19(5):672–81.
[29] Tawbi HA, Forsyth PA, Algazi A, Hamid O, Hodi FS, Moschos SJ, et al. Combined nivolumab and ipilimumab in melanoma metastatic to the brain. N Engl J Med 2018;379(8):722–30.